Two novel pleiotropic loci associated with osteoporosis and abdominal obesity

Lu Liu[1,2,3], **Xiao-Lin Yang**[1,2], **Hong Zhang**[1,2], **Zi-Jia Zhang**[4], **Xin-Tong Wei**[2,5], **Gui-Juan Feng**[2,5], **Ju Liu**[3], **Hui-Ping Peng**[3], **Rong Hai**[6], **Hui Shen**[7], **Qing Tian**[7], **Hong-Wen Deng**[7], **Yu-Fang Pei**[2,5], **Lei Zhang**[1,2]

[1]Center for Genetic Epidemiology and Genomics, School of Public Health, Medical College, Soochow University, 199 Ren-ai Rd, Suzhou 215123, Jiangsu, People's Republic of China

[2]Jiangsu Key Laboratory of Preventive and Translational Medicine for Geriatric Diseases, School of Public Health, Medical College of Soochow University, Suzhou, Jiangsu, People's Republic of China

[3]Kunshan Hospital of Traditional Chinese Medicine, Suzhou, Jiangsu, People's Republic of China

[4]People's Hospital of Inner Mongolia Autonomous Region, Hohhot, Inner Mongolia Autonomous Region, People's Republic of China

[5]Department of Epidemiology and Health Statistics, School of Public Health, Medical College, Soochow University, 199 Ren-ai Rd., Suzhou 215123, Jiangsu, People's Republic of China

[6]Health Commission of Inner Mongolia Autonomous Region, Hohhot, Inner Mongolia Autonomous Region, People's Republic of China

[7]Tulane Center for Genomics and Bioinformatics, Department of Biostatistics and Bioinformatics, School of Public Health and Tropical Medicine, Tulane University, 1440 Canal St., Suite 2001, New Orleans, LA 70112, USA

Abstract

Aiming to uncover a shared genetic basis of abdominal obesity and osteoporosis, we performed a bivariate GWAS meta-analysis of femoral neck BMD (FNK-BMD) and trunk fat mass adjusted by

trunk lean mass (TFM$_{adj}$) in 11,496 subjects from 6 samples, followed by in silico replication in the large-scale UK Biobank (UKB) cohort. A series of functional investigations were conducted on the identified variants. Bivariate GWAS meta-analysis identified two novel pleiotropic loci 12q15 (lead SNP *rs73134637*, $p = 3.45 \times 10^{-7}$) and 10p14 (lead SNP *rs2892347*, $p = 2.63 \times 10^{-7}$) that were suggestively associated and that were replicated in the analyses of related traits in the UKB sample (osteoporosis $p = 0.06$ and 0.02, BMI $p = 0.03$ and 4.61×10^{-3}, N up to 499,520). *Cis*-eQTL analysis demonstrated that allele C at *rs73134637* was positively associated with *IFNG* expression in whole blood ($N = 369$, $p = 0.04$), and allele A at *rs11254759* (10p14, $p = 9.49 \times 10^{-7}$) was negatively associated with *PRKCQ* expression in visceral adipose tissue ($N = 313$, $p = 0.04$) and in lymphocytes ($N = 117$, $p = 0.03$). As a proof-of-principle experiment, the function of *rs11254759*, which is 235 kb 5′-upstream from *PRKCQ* gene, was investigated by the dual-luciferase reporter assay, which clearly showed that the haplotype carrying *rs11254759* regulated *PRKCQ* expression by upregulating *PRKCQ* promoter activity ($p = 4.60 \times 10^{-7}$) in an allelic specific manner. Mouse model analysis showed that heterozygous *PRKCQ* deficient mice presented decreased fat mass compared to wild-type control mice ($p = 3.30 \times 10^{-3}$). Mendelian randomization analysis demonstrated that both FNK-BMD and TFM$_{adj}$ were causally associated with fracture risk ($p = 1.26 \times 10^{-23}$ and 1.18×10^{-11}). Our findings may provide useful insights into the genetic association between osteoporosis and abdominal obesity.

Introduction

Osteoporosis is a chronic metabolic disease characterized by low bone mineral density (BMD) and deficiencies in the structure of bone tissue. It reduces bone strength and increases the risk of fracture (Notelovitz 1993) and is a major public health problem, conferring substantial morbidity and mortality and affecting over 200 million people worldwide, particularly postmenopausal women (Aaseth et al. 2012). At least 16% of US adults above the age of 65 report clinical symptoms of osteoporosis at either the lumbar spine or femoral neck (Looker and Frenk 2015).

Obesity is another chronic metabolic disease characterized by an excessive accumulation of body fat. It is one of the most severe public health problems, associated with a series of disorders including diabetes, cancer, cardiovascular disease, osteoarthritis, and obstructive sleep disease (Haslam and James 2005). Among various types of fat-induced obesity, abdominal obesity is perhaps the most severe. It is well established that fat stored at the abdomen is more harmful than fat stored at other body regions. For example, truncal adiposity confers a threefold increased risk for heart disease in women compared with the accumulation of body fat in the gluteal femoral region (Rexrode et al. 1998). Moreover, fat mass stored more centrally leads people to be more susceptible to cardiovascular diseases and endocrine disorders (Pischon et al. 2008).

Both osteoporosis and obesity have strong genetic determinants. For example, the reported heritability for bone mineral density (BMD) and body mass index (BMI), the standard major predictor for the two diseases, is estimated at 50–90% (Deng et al. 2000) and > 40% (Fall and Ingelsson 2014; Maes et al. 1997; Zaitlen et al. 2013), respectively. Hundreds of genomic loci associated with BMD and BMI have been identified through a number of

genome-wide association studies (GWASs) and their meta-analyses (Estrada et al. 2012; Kemp et al. 2017; Locke et al. 2015; Medina-Gomez et al. 2018; Pei et al. 2014; Zheng et al. 2015).

Obesity and osteoporosis have specific pathogenesis and a shared biological basis (Zhao et al. 2007). Adipocytes and osteoblasts originate from a shared progenitor bone marrow mesenchymal stem cells, and both cells can transdifferentiate into each other (Gimble et al. 1996). The factors secreted by adipocytes, such as estrogen synthesis enzyme, aromatase, leptin and various proinflammatory cytokines, play important roles in bone remodeling (Gimble et al. 1996). On the other hand, some bone-derived factors, such as osteopontin and osteocalcin, are able to regulate body weight and glucose homeostasis at the endocrine level (Gomez-Ambrosi et al. 2008). The biological crosstalk between bone and fat implies pleiotropic genes regulating both traits. Previous studies have identified a number of loci and candidate genes, such as *SOX6* (Liu et al. 2009), *MARK3, DNM3, CDKAL1, MPP7* (Hu et al. 2018) and *FTO* (Guo et al. 2011). Despite these findings, more pleiotropic loci underlying osteoporosis and obesity remain undiscovered.

In the present study, we aim to identify pleiotropic loci for abdominal obesity and osteoporosis by performing a large scale bivariate GWAS meta-analysis of femoral neck BMD (FNK-BMD) and trunk fat mass adjusted by trunk lean mass (TFM_{adj}) in 11,496 subjects. We then replicated the results in the large-scale UK biobank (UKB) cohort sample. As a proof-of-principle experiment, we conduct dual-luciferase assay on the identified locus 10p14 to investigate the functional relevance of the associated variants. We then survey mouse knockout models to evaluate bone-related or fat-related phenotypic consequence of the susceptible genes. Fianally, we perform a Mendelian randomization analysis to investigate the possibility of causal relationships between obesity, osteoporosis, and other metabolic diseases.

Materials and methods

Study population

Six GWAS samples were incorporated into our study: three from in-house studies and three accessed through the NCBI Database of Genotypes and Phenotypes (dbGAP). The in-house samples included two consisting of samples from European populations, with 1000 (the Omaha Osteoporosis Study, OOS) and 2286 (the Kansas City osteoporosis study, KCOS) unrelated individuals, and one study of a Chinese Han population with 1627 unrelated individuals (the China osteoporosis study, COS) (Zhang et al. 2014a). The fourth sample was derived from the Framingham Heart Study (FHS), a longitudinal and prospective cohort comprising over 16,000 participants of European ancestry spanning three generations (Rivadeneira et al. 2009). A total of 5969 phenotyped individuals were included. Both the fifth and sixth samples were derived from the Women's Health Initiative (WHI) observational study, a partial factorial randomized and longitudinal cohort with over 12,000 genotyped women, aged 50–79 years, of African-American or Hispanic ancestry (The Women's Health Initiative Study Group 1998). The fifth sample comprises 847 phenotyped individuals of African-American ancestry (WHI-AA), and the sixth sample comprises 445 phenotyped individuals of Hispanic ancestry (WHI-HIS).

Phenotype measurements and modeling

BMD and TFM were measured by dual-energy X-ray absorptiometry (DXA) bone densitometers (either Lunar Corp., Madison, WI, USA; or Hologic Inc, Bedford, MA, USA). For TFM, covariates including gender, age, age^2, height, height^2 and the first five principal components (PCs) derived from genome-wide genotype data were screened for significance with the stepwise linear regression model implemented in the *stepAIC* function of R package MASS. To adjust the effect of lean mass, trunk lean mass was taken as a covariate as well. Regression residuals were transformed into a standard normal distribution using the inverse quantiles of standard normal distribution. Normalized residuals were used for subsequent association analysis. For FNK-BMD, covariates including gender, age, age^2, height, and the first five PCs derived from genome-wide genotype data were screened for significance with the step-wise linear regression model implemented in the R function *stepAIC*. Raw BMD and TFM values were adjusted by significant covariates, and the residuals were normalized by inverse quantiles of standard normal distribution. Phenotypic correlation between BMD and TFM was calculated based on raw phenotypes in each individual study.

Genotyping and quality control

All GWAS samples were genotyped by high-throughput single-nucleotide polymorphism (SNP) genotyping arrays (Affymetrix Inc, Santa Clara, CA, USA; or Illumina Inc., San Diego, CA, USA within individual samples) according to the manufacturers' protocols. Quality control (QC) within each sample was implemented at both the individual and SNP levels. At the individual level, sex compatibility was checked by imputing sex from X-chromosome genotype data with PLINK (Purcell et al. 2007). Individuals of ambiguous imputed sex or of imputed sex inconsistent with reported sex were removed. At the SNP level, SNPs violating the Hardy–Weinberg Equilibrium (HWE) rule (p value $< 1.0 \times 10^{-5}$) were removed. Genotypes presenting the Mendel error were set to missing in the familial sample.

Genotype imputation

GWAS samples were imputed to the 1000 Genomes Project phase 3 sequence variants (as of May 2013) (Genomes Project et al. 2010). Genotype imputation reference panels of 503 individuals of European ancestry, 504 individuals of East Asian ancestry, 661 of African ancestry, and 347 of admixed American ancestry were downloaded from the project website. Each GWAS sample was imputed by its respective reference panel with the closest ancestry. Haplotypes of bi-allelic variants, including SNPs and bi-allelic insertions/deletions (indels), were extracted to form reference panels for imputation. As a QC procedure, variants with zero or one copy of minor alleles were removed.

Prior to imputation, a consistency test of allele frequency between the GWAS sample and the reference sample was examined with the Chi-square test. To correct for potential mis-strandedness, GWAS SNPs that failed the consistency test ($p < 1.0 \times 10^{-6}$) were transformed into the reverse strand. SNPs that again failed the consistency test were removed from the GWAS sample.

Imputation was performed with FISH, an algorithm we developed to impute the diploid genome without the need to phase genotype into haplotype (Zhang et al. 2014b). The imputation accuracy was measured by the imputation certainty score r^2, which is defined as the correlation between imputed dosage and the best-imputed genotype. Variants of low imputation accuracy ($r^2 < 0.3$) were excluded from subsequent analyses.

Individual study association test

Each GWAS sample was tested for association between normalized phenotype residuals and genotyped and imputed genotypes, under an additive mode of inheritance. Both univariate and bivariate association tests were performed in each individual sample. In the FHS sample, both univariate and bivariate associations were examined within a linear mixed model to account for genetic relatedness within each pedigree (Zhang et al. 2009a, b). For the unrelated samples, both univariate and bivariate association tests were examined with a linear regression model. All the analyses were performed by the in-house program GAP, as described previously (Zhang et al. 2009c).

Meta-analysis

Summary association statistics from individual GWAS samples were combined to perform univariate or bivariate meta-analyses. As a QC procedure, only common or less common (MAF > 0.01 in the European population) and well-imputed ($r^2 > 0.3$ in at least two samples) SNPs were included for analysis.

Both univariate and bivariate meta-analyses were performed under the inverse variance weighted fixed-effects model (Konstantopoulos 2006). Briefly, for a particular SNP, let (β_{1i}, β_{2i}) be the regression coefficients for the two traits in the study ($i = 1, \ldots, n$, $N = 6$), and let $\mathbf{V}_i = \begin{bmatrix} v_{11} & v_{12} \\ v_{21} & v_{22} \end{bmatrix}$ be the corresponding symmetric variance–covariance matrix for the two regression coefficients. Both β_{1i}, β_{2i} and V_i are obtained from the individual study analysis. Define the following data structure $\mathbf{B} = (\beta_{11}, \beta_{21}, \beta_{12}, \beta_{22}, \ldots, \beta_{1n}, \beta_{2n})'_{2n \times 1}$.

$$\mathbf{X} = \begin{bmatrix} 1 & 0 \\ 0 & 1 \\ \cdots \\ 1 & 0 \\ 0 & 1 \end{bmatrix}_{2n \times 2}, \mathbf{V} = \begin{bmatrix} \mathbf{V}_1 & & & \\ & \mathbf{V}_2 & & \\ & & \cdots & \\ & & & \mathbf{V}_n \end{bmatrix}_{2n \times 2n}$$, where $\mathbf{B}$ is the vector of the regression coefficient, $\mathbf{X}$

is the design matrix, and $\mathbf{V}$ is the variance–covariance matrix for all studies, respectively.

The generalized least-squared estimator $\widehat{\boldsymbol{\beta}}$ of overall regression coefficients is given by $\widehat{\boldsymbol{\beta}} = \left(\mathbf{X}'\mathbf{V}^{-1}\mathbf{X} \right)^{-1} \mathbf{X}'\mathbf{V}^{-1}\mathbf{B}$, which has a normal distribution with mean $\boldsymbol{\beta}$ and covariance matrix $\boldsymbol{\Sigma}$ given by,

$$\boldsymbol{\Sigma} = \left(\mathbf{X}'\mathbf{V}^{-1}\mathbf{X} \right)^{-1}.$$

Under the null hypothesis of no association to either phenotype, that is, $\boldsymbol{\beta} = \mathbf{0}$ (for both traits), the score statistic

$$T_{12} = \hat{\boldsymbol{\beta}}' \boldsymbol{\Sigma}^{-1} \hat{\boldsymbol{\beta}}$$

will asymptotically follow a chi-squared distribution with 2 degrees of freedom. The two univariate test-statistics are constructed similarly. Specifically,

$$T_1 = \frac{\hat{\boldsymbol{\beta}}_1^2}{\boldsymbol{\Sigma}_{11}}, \quad T_2 = \frac{\hat{\boldsymbol{\beta}}_2^2}{\boldsymbol{\Sigma}_{22}},$$

where $\hat{\boldsymbol{\beta}}_1$ and $\hat{\boldsymbol{\beta}}_2$ are two elements in $\hat{\boldsymbol{\beta}}$, and $\boldsymbol{\Sigma}_{11}$ and $\boldsymbol{\Sigma}_{22}$ are two diagonal elements in $\boldsymbol{\Sigma}$. Under the null hypothesis of no univariate association, that is, $\boldsymbol{\beta}_1 = 0$ or $\boldsymbol{\beta}_2 = 0$, T_1 or T_2 will follow a chi-squared distribution with 1 degree of freedom. The above meta-analysis model was implemented in an in-house java program *BiMeta.jar*, which is available upon request to the corresponding authors.

To monitor potential genetic heterogeneity due to difference of allele frequency in samples of different ethnic populations, the Cochran's Q p value from the two univariate association results was reported.

Replication in the UKB summary results

To replicate the association signals of our identified SNPs, we performed in silico replication of related traits in the UKB cohort sample by surveying the Gene ATLAS web portal (Canela-Xandri et al. 2018), a large database of associations between hundreds of traits and millions of variants using the UK Biobank (UKB) cohort (https://geneatlas.roslin.ed.ac.uk/). Successful replication was declared at a nominal significant p value ($p < 0.05$) and consistent effect direction.

Functional annotation

We evaluated the functional relevance of the identified SNPs and their proxy SNPs (r^2 0.7) using data from the ENCODE project, which includes a diverse set of 15 chromatin marks assayed in multiple cell types, such as H3K4me3, H3K4me1, H3K27ac and Dnase hypersensitivity site (DHS) (ENCODE Project Consortium 2011). Annotations were performed via the Haploreg web portal (Ward and Kellis 2012).

Fine-mapping

We fine-mapped plausibly causal variants at the identified loci with FINEMAP (Benner et al. 2016), which uses GWAS summary statistics to explore a set of the most important causal configurations in the target region via a shotgun stochastic search algorithm. The input of FINEMAP includes univariate association statistics (regression coefficient and its standard error) and a reference LD panel. We evaluated the two individual traits in turn using univariate association statistics. LD was estimated based on the 1000 Genomes Project European sample. The maximal number of causal SNPs was set to the default number 5.

Cis-expression quantitative trait loci (cis-eQTL) analysis

To investigate the association between the identified SNP polymorphisms and nearby gene expressions, we performed *cis*-eQTL analysis. The datasets we used were derived from the Genotype-Tissue Expression (GTEx) project (GTEx Consortium 2013). The GTEx project collected RNA-sequenced multiple human tissues (up to 11,614) from donors who were also densely genotyped, and searched for associations between SNPs and global RNA expression within individual tissues. We analyzed whole blood ($N = 369$) and three tissues related to both obesity and osteoporosis: subcutaneous adipose tissue ($N = 385$), visceral adipose tissue ($N = 313$) and lymphocytes ($N = 117$).

Dual-luciferase reporter assay

As a proof-of-principle experiment, we conducted a dual-luciferase reporter assay to evaluate whether the three neighboring variants (*rs11254759*, *rs11254758* and *rs11254760*) at 10p14 regulate the expression of *PRKCQ* (Protein Kinase C Theta) gene. Human embryonic kidney cell line 293 T (HEK293T cells) were cultured in DEME high glucose (Hyclone, Thermo Fisher Scientific Inc.) supplemented with 10% fetal bovine serum (FBS, Tianhang Inc.), 100 U mL^{-1} penicillin, and 100 μg mL^{-1} streptomycin. Cells were maintained at 37 °C in a water-saturated atmosphere under 5% CO_2 in air and were cultured to 60%−80% in 12-well culture plate before transfection.

Luciferase reporter plasmid containing *PRKCQ* promoter was constructed by inserting a 2046 bp sequence containing *PRKCQ* promoter (ENST00000263125.5; *PRKCQ*-001) into the *MluI* and *XhoI* sites of the pGL3-basic vector (Promega Corporation, Madison, WI, USA), which expresses the *Firefly* luciferase gene. This pGL3-PRKCQ-Promoter construct served as a negative control. For the experimental group, a 312 bp DNA sequence containing three SNPs (*rs11254758*, *rs11254759* and *rs11254760*) was cloned into the 5′-end of the above pGL3-PRKCQ-Promoter vector, forming the pGL3-SNP-SNPs-Promoter construct. Based on the results of *cis*-eQTL, we cloned two types of sequence, each containing either trait-raising alleles (*rs11254758*-G, *rs11254759*-G, *rs11254760*-T) or trait-lowering alleles (*rs11254758*-A, *rs11254759*-A, *rs11254760*-C). The success of plasmid construction was confirmed by DNA Sanger sequencing. The construct was then transfected into the 293 T cells using the jetPRIME transfection reagent (PolyPlus-transfection, France). As an internal control for transfection efficiency, the pRL-TK vector (Promega Corporation, Madison, WI, USA) expressing the *Renilla* luciferase gene was co-transfected at the same time. The cells were collected for luciferase activity measurement after 24 h of transfection. We conducted four experiment replicates under each condition.

Luciferase activity was measured using the dual-luciferase reporter system (Promega Corporation, Madison, WI, USA) following the manufacturer's instructions. The ratio of *Firefly* to *Renilla* luciferase activity was compared between the pGL3-SNPs-PRKCQ-Promoter construct and the pGL3-PRKCQ-Promoter control construct. We also compared the control construct with the null pGL3-basic vector containing no *PRKCQ* promoter to examine the transcription efficacy of the promoter and compared between two allelic experiment groups. Statistical significance was tested using an unpaired Student's *t* test.

Mouse model survey

We surveyed mouse knockout models to evaluate bone- or fat-related phenotypic consequences of *IFNG* and *PRKCQ*, including changes in BMD, bone mineral content (BMC), body weight, and fat mass. We primarily searched the International Mouse Phenotyping Consortium (IMPC) database via its web portal (https://www.mousephenotype.org/) (Dickinson et al. 2016).

Mendelian randomization analysis (MR analysis)

Finally, we performed a Mendelian randomization analysis to investigate the causal relationship between the two studied traits and other metabolic disorders. We used the software GSMR (Zhu et al. 2018), which uses GWAS summary statistics to establish a causal association from an exposure to an outcome using signed regression coefficient and its standard error. We evaluated each trait, in turn, using univariate GWAS summary statistics. For each trait, we evaluated the causality to nine selected metabolic disorders, including fracture, amyotrophic lateral sclerosis (ALS), autistic spectrum disorder (ASD), type 2 diabetes (T2D), insomnia, inflammatory bowel disease (IBD), smoking addiction, coronary artery disease (CAD), and bipolar disorder.

GWAS summary statistics for these diseases were downloaded from their respective websites. From the list of SNPs whose association signals with the exposure trait were below 1.0×10^{-5}, qualified SNPs were included based on the following criteria: concordant alleles between exposure and outcome GWAS summary statistics, non-palindromic SNPs with certain strands, MAF > 1%, and allele frequency difference between exposure and outcome GWAS summary statistics < 0.2.

Independent SNPs were further clumped with PLINK2 (Chang et al. 2015) with independence LD threshold $r^2 < 0.05$ and 1 MB window size. For each pair of exposure-outcome traits, the clumped independent SNPs were examined for their pleiotropic effects to both exposure and outcome using the HEIDI test (Zhu et al. 2018). Significance level for the HEIDI test was set to $a = 1.0 \times 10^{-5}$. After removing pleiotropic SNPs on an outcome-by-outcome basis, the remaining independent SNPs were taken as instrumental variables to test for the causal effect of exposure to outcome. Significance level was set to 5.56×10^{-3} (0.05/9).

Results

Meta-analysis

Basic characteristics of the GWAS meta-analysis samples are listed in Table 1. Principal component analysis (PCA) was applied to each individual sample, and no population outlier was observed. A total of 28,855,047 bi-allelic variants were imputed into the 1000 Genomes Project reference panel. After filtering out rare variants and variants of poor imputation certainty, 12,061,510 variants were retained for association analysis. After adjusting the phenotype by PCA in each individual study, the genomic control inflation factor was small ($\lambda = 1.04$), indicating the limited effect of population stratification. A logarithmic quantile–

quantile (QQ) plot of meta-analysis test statistics shows a marked deviation in the tail of the distribution, suggesting the possible existence of true association (Supplementary Fig. 1).

In univariate meta-analysis, three loci were associated with TFM_{adj} at the genome-wide significance level (GWS, $p < 5.0 \times 10^{-8}$): 1p21 ($rs12409479$, $p = 4.75 \times 10^{-10}$), 8q21 ($rs2091921$, $p = 2.09 \times 10^{-10}$) and 20p11 ($rs4813371$, $p = 8.92 \times 10^{-9}$). Two loci were associated with FNK-BMD at the GWS level: 1p31 ($rs140423501$, $p = 4.59 \times 10^{-8}$) and 5q14 ($rs36088869$, $p = 2.53 \times 10^{-8}$) (Supplementary Fig. 2). The main results of univariate meta-analysis are displayed in Supplementary Table 1. All these loci have been reported by previous GWAS studies (Duncan et al. 2011; Kemp et al. 2017).

The bivariate meta-analysis identified four loci, 1p21 ($rs12409479$, bivariate $p = 3.63 \times 10^{-9}$), 5q14 ($rs36088869$, bivariate $p = 4.05 \times 10^{-8}$), 8q21 ($rs2091921$, bivariate $p = 3.03 \times 10^{-9}$) and 18p11 ($rs78202598$, bivariate $p = 1.33 \times 10^{-8}$), associated bivariately at the GWS level (Fig. 1).

At the suggestive significance threshold ($p < 1.0 \times 10^{-6}$), a total of 18 genomic loci were identified by bivariate GWAS meta-analysis. Of those, eight loci were associated with both traits at the nominal significance level ($p < 0.05$), and were defined as pleiotropic loci. (Supplementary Table 2).

Five (6p21, 10q23, 1q31, 17p13 and 18p11) of the above eight pleiotropic loci have been identified for either osteoporosis or obesity traits by previous GWAS studies (Estrada et al. 2012; Kim 2018; Locke et al. 2015; Morris et al. 2019). The remaining three loci, 10p14 (lead SNP, $rs2892347$, bivariate $p = 2.63 \times 10^{-7}$), 12q15 (lead SNP, $rs73134637$, bivariate $p = 3.45 \times 10^{-7}$) and 13q31 (lead SNP, $rs369240153$, bivariate $p = 2.70 \times 10^{-7}$), are novel to both traits.

Replication results in UKB samples

The three novel pleiotropic loci were subjected to in silico replication in the UKB GWAS summary results of related traits. $rs2892347$ is significant for osteoporosis ($p = 0.02$, $N = 383,478$) and BMI ($p = 4.61 \times 10^{-3}$, $N = 499,520$). $rs73134637$ is significant for trunk fat percentage ($p = 0.03$, $N = 492,388$) and nearly significant for osteoporosis without pathological fracture ($p = 0.06$, $N = 410,289$). Finally, $rs369240153$ is not significant for any related traits. Both $rs2892347$ and $rs73134637$ are also consistent in effect direction, strengthening the evidence of true association. The main results of the two novel loci are listed in Table 2. The effect allele frequency (EAF) across different samples for the lead SNPs of two novel loci are listed in Supplementary Table 3. The forest plots are displayed in Fig. 2, and the regional plots are drawn by LocusZoom (Pruim et al. 2010) are shown in Supplementary Fig. 3.

Functional annotation

We annotated $rs2892347$ and $rs73134637$ and their neighboring SNPs (LD r^2 0.7) through HaploReg (Ward and Kellis 2012). $rs73134637$ has enhancer activities as predicted by enhancer histone mark 7_Enh and 17_EnhW2 in chondrocyte cells, and also coincides with enhancer markers (7_Enh and H3K4me1_Enh) in mesenchymal stem cells and osteoblast

primary cells. $rs11254759$ (bivariate $p = 9.49 \times 10^{-7}$) and its two proxy SNPs ($rs11254758$ and $rs11254760$, bivariate $p = 1.39 \times 10^{-6}$ and 1.32×10^{-6}, respectively), which are in modest level LD with $rs2892347$ ($r^2 = 0.7$), are located in evolutionarily conserved regions as predicted by both GERP and SiPhy. They all have enhancer activities as predicted by enhancer histone marks 7_Enh and H3K4me1_Enh in mesenchymal stem cells and osteoblast primary cells.

Fine-mapping

We next performed fine-mapping analysis to prioritize plausible causal variants at the identified loci.

At 10p14, the set of most probably causal SNPs is ($rs12771874$, $rs188462291$, $rs112816298$, $rs10905103$ and $rs78967739$) using FNK-BMD summary statistics. Notably, the LD level between all pairs of these SNPs is weak, indicating each of them represents a distinct association signal. Using TFM$_{adj}$ summary statistics, the set is ($rs11254803$, $rs200579923$, $rs17141967$, $rs10905040$ and $rs10458799$). In contrast, these SNPs are in strong LD level with each other, but they are in very weak LD with the five SNPs in the FNK-BMD set, implying that the two sets are from different association sources.

At 12q15, the set inferred from FNK-BMD is ($rs73134637$, $rs2956534$, $rs7309010$, $rs12313946$ and $rs2860493$), and that from TFM$_{adj}$ is ($rs11833102$, $rs10784734$, $rs1152937$, $rs2120743$ and $rs2453750$).

Cis-eQTL analysis

We then performed *cis*-eQTL analysis in subcutaneous adipose tissue, visceral adipose tissue, lymphocytes and whole blood of the GTEx project datasets. The results show that $rs73134637$ polymorphisms are significantly associated with *IFNG* gene expression in whole blood. Specifically, allele C is associated with a higher level of gene expression ($p = 0.04$, $N = 369$). This association is not observed in any of the other three tissues. $rs11254759$ polymorphisms are significantly associated with *PRKCQ* expression in visceral adipose tissue ($p = 0.04$, $N = 313$) and in lymphocytes ($p = 0.03$, $N = 117$). Specifically, allele G is associated with an increased level of *PRKCQ* expression.

Dual-luciferase reporter assay

As a proof-of-principle experiment, we evaluated the regulation of $rs11254759$ (and its two proxy SNPs) to *PRKCQ* gene expression.

We conducted a dual-luciferase reporter assay in HEK293T cells. Specifically, pGL3-PRKCQ-Promoter construct served as a negative control. The three correlated SNPs ($rs11254759$, $rs11254758$ and $rs11254760$) are located close together and in high LD ($r^2 = 1.0$). Moreover, *cis*-eQTL analysis shows that the three SNPs are all associated with the level of *PRKCQ* expression in an allele-specific manner. Thus, to achieve the strongest luciferase effect, a 312 bp DNA fragment combining three SNPs was cloned into the luciferase reporter vector containing *PRKCQ* promoter. These constructs were transfected into HEK293T cells along with pRL-TK vector.

The luciferase reporter assay results are displayed in Fig. 3. Compared to the null pGL3-basic vector, the control vector containing the *PRKCQ* promoter significantly increases luciferase activity by about twofold ($p = 4.60 \times 10^{-7}$), proving the successful construction of the *PRKCQ* promoter in promoting luciferase gene expression. Compared to the pGL3-PRKCQ-Promoter vector, the pGL3-SNPs-PRKCQ-Promoter vector containing either trait-raising alleles (*rs11254759*-G, *rs11254758*-G, *rs11254760*-T) or trait-lowering alleles (*rs11254759*-A, *rs11254758*-A, *rs11254760*-C) increases *PRKCQ* expression ($p = 0.10$ or 0.002), though the increment magnitude is minor. This result suggests that the sequence containing three variants could upregulate *PRKCQ* gene expression by promoting *PRKCQ* promoter activity. Between the two constructs, the expression of trait-raising alleles is slightly higher than that of trait-lowering alleles ($p = 0.01$), implying that the regulation is allele-specific.

IMPC survey results

Compared with wild-type control mice, heterozygous *PRKCQ* deficiency mice have a decreased fat mass phenotype ($p = 3.30 \times 10^{-3}$) and heterozygous *IFNG* deficiency mice demonstrate increased body weight ($p = 1.49 \times 10^{-3}$). However, the difference in BMD/BMC between wild-type and gene-deficient mice is not significant for both genes.

MR analysis

To investigate whether BMD or TFM is causally linked with other complex diseases, a Mendelian randomization analysis was performed. At the corrected significance level 5.56×10^{-3} (0.05/9), both traits are causally associated with fracture risk (FNK-BMD $p = 1.26 \times 10^{-23}$; TFM$_{adj}$ $p = 1.18 \times 10^{-11}$), but not with any other disease (Supplementary Table 4).

Discussion

In the present study, we performed a bivariate genome-wide association meta-analysis of FNK-BMD and TFM$_{adj}$ in 11,496 participants from six GWAS samples, and have identified two novel pleiotropic loci at the suggestive significance level. Moreover, the role of *rs11254759* at 10p14 related to bone and fat development has been investigated by a series of functional investigations.

Currently, hundreds of genomic loci for obesity and osteoporosis have been mapped by massive GWAS analyses, which were generally focused on individual traits. Bivariate analysis has a high statistical power in identifying associated variants not found by univariate approaches. Previous studies on association tests of multiple correlated traits have shown that they improve the statistical power to evaluate the effects of pleiotropic genes that jointly influence complex traits (Liu et al. 2009; Tan et al. 2015). By performing a bivariate GWAS meta-analysis, we not only identified pleiotropic loci that have previously reported associations with obesity and osteoporosis (Estrada et al. 2012; Locke et al. 2015), such as 17p13 (*rs8072532*, bivariate $p = 4.77 \times 10^{-7}$) but also identified novel pleiotropic loci, such as 10p14 (lead SNP, *rs2892347*, bivariate $p = 2.63 \times 10^{-7}$) and 12q15 (lead SNP, *rs73134637*, bivariate $p = 3.45 \times 10^{-7}$).

Though the relationship between obesity and osteoporosis has been extensively studied, evidence for the genetic association between abdominal obesity and osteoporosis is sparse. Abdominal fat is located in two major compartments: subcutis and viscera. Visceral adiposity is highly associated with increased risk of type 2 diabetes, dyslipidemia, and thrombosis in the heart (CVD), arties, veins, or capillaries (Booth et al. 2014). In this study, the pleiotropic variant *rs11254759* at 10p14 was identified, whose polymorphisms were significantly associated with *PRKCQ* expression in visceral adipose tissue ($N = 313$, $p = 0.04$) and lymphocytes ($p = 0.03$, $N = 117$). *rs11254759* is located 233 kb upstream of *PRKCQ* gene. It is worth noting that both *rs11254759* and its proxy SNPs (*rs11254758* and *rs11254760*) have enhancer activities in adipose-derived mesenchymal stem cells and osteoblast primary cells. The dual-luciferase reporter assay results suggest that the sequence containing the three variants could upregulate *PRKCQ* gene expression by promoting *PRKCQ* promoter activity. Mouse model surveys showed that *PRKCQ* deficiency could lead to decreased fat mass in mice. *PRKCQ* has been found to inhibit the expression of estrogen receptor alpha (ER-α), a major receptor of estrogen and a well recognized factor regulating both obesity and bone (Bu et al. 2009). Altogether, combining the evidence from the genetic association analyses and the bioinformatical and functional investigations, we hypothesize that the pleiotropic variant *rs11254759* and its proxy SNPs may influence trunk fat mass and BMD by regulating *PRKCQ* promoter activity in visceral adipose tissue/lymphocytes.

Heterozygous *IFNG* deficiency mice showed increased body weight ($p = 1.49 \times 10^{-3}$) compared to wild-type controls. In addition, IFNG-KO has systemic effects on adiposity, including improved insulin sensitivity and decreased adipocyte size in obese mice (O'Rourke et al. 2012). However, there is little biological evidence on the function of *IFNG* in bone development. In this study, another novel pleiotropic variant *rs73134637* (12q15, bivariate $p = 3.45 \times 10^{-7}$), whose polymorphisms exerted *cis*-effects on the expression of the gene *IFNG* in whole blood ($p = 0.04$, $N = 369$), has enhancer activities in bone-related cells (mesenchymal stem cells, and osteoblast primary cells and chondrocyte cells). The results may provide clues for subsequent investigation on the role of *IFNG* in bone development.

Although the relationship of obesity with fracture has been explored widely by many epidemiological studies, one controversial question is whether obesity exerts a protective against the effect on fracture. Some studies suggested that obesity was protective against fractures as a result of protection by soft tissue padding against falls (Compston 2013). In a prospective study, the individuals with the lowest quartiles of fat mass presented an increased risk of hip fracture (Ensrud et al. 1997). However, some other findings reported the opposite results. For example, a large Chinese cohort study showed that non-spine fractures were significantly higher in subjects with a higher percentage of body fat, independent of body weight (Gonnelli et al. 2014; Hsu et al. 2006). In the present study, we found that genetically increased TFM_{adj} was causally associated with increased fracture risk using MR analysis of GWAS summary statistics ($p = 1.18 \times 10^{-11}$, $\beta = 0.42$), which strengthen the evidence that abdominal obesity might be one of the risk factors for fracture.

The samples that we analyzed were diverse in ancestries. Different race/ethnic populations might, but do not necessarily result in genetic heterogeneity. Though the random-effects model is more robust to heterogeneity, it is over-conservative. Only when a significant

heterogeneity effect is detected then a random-effects model would be applied. By convention, we performed GWAS meta-analyses under a fixed-effects model. In our study, genetic heterogeneity was monitored by univariate Cochran's Q p value, which was > 0.05 at both two identified lead SNPs. This indicates that genetic heterogeneity from different samples has a limited effect on the association results.

Certain limitations exist in the present study. First, the *cis*-eQTL analysis of the identified SNPs for osteoporosis was conducted in lymphocytes. In fact, the study was limited due to the current lack of biological data publicly available for osteoblasts and osteoclasts, making it necessary for us to choose alternative cells/tissues related to osteoporosis. Lymphocytes are associated with bone development. For example, B-lymphocytes could regulate osteoporosis development through expressing/secreting factors involved in osteoclastogenesis, such as receptor tumor necrosis factor superfamily member 11 (*TNFSF11*) and osteoprotegerin (Manabe et al. 2001; Mullin et al. 2018). Second, the dual-luciferase assay could identify variants regulating gene expression by affecting gene promoter activity, but not the specific regulation mechanism. Experiments with finer resolution, such as DNA pull-down assay followed by protein mass spectrum or super-sift assay with a hypothesized protein antibody, may identify the specific effect mechanism, which is out of the scope of the present study.

In conclusion, by performing a bivariate genome-wide association meta-analysis of TFM_{adj} and FNK-BMD in 11,496 subjects from six samples, we have identified two novel pleiotropic genetic loci simultaneously associated with TFM_{adj} and FNK-BMD, and have suggested their biological effects in bone and trunk fat development. Our study could improve the understanding of the genetic basis of abdominal obesity and osteoporosis risk and the genetic correlation between both diseases.

Supplementary Material

Refer to Web version on PubMed Central for supplementary material.

Acknowledgements

Author Manuscript

Author Manuscript

Author Manuscript

Author Manuscript

References

Aaseth J, Boivin G, Andersen O (2012) Osteoporosis and trace elements—an overview. J Trace Elem Med Biol 26:149–152. 10.1016/j.jtemb.2012.03.017 [PubMed: 22575536]

Benner C, Spencer CC, Havulinna AS, Salomaa V, Ripatti S, Pirinen M (2016) FINEMAP: efficient variable selection using summary data from genome-wide association studies. Bioinformatics 32:1493–1501. 10.1093/bioinformatics/btw018 [PubMed: 26773131]

Booth A, Magnuson A, Foster M (2014) Detrimental and protective fat: body fat distribution and its relation to metabolic disease. Horm Mol Biol Clin Investig 17:13–27. 10.1515/hmbci-2014-0009

Bu F-X, Zhao L-J, Pei Y-F, Recker R, Deng H-W (2009) Powerful bivariate genome-wide association analyses and follow-up replication studies identified several pleitropic genes for both obesity and femoral neck geometry. ASBMR 31st Annual Meeting FR0001–FR0464. J Bone Miner Res 24:S94–S149. 10.1002/jbmr.5650241302

Canela-Xandri O, Rawlik K, Tenesa A (2018) An atlas of genetic associations in UK Biobank. Nat Genet 50:1593–1599. 10.1038/s41588-018-0248-z [PubMed: 30349118]

Chang CC, Chow CC, Tellier LC, Vattikuti S, Purcell SM, Lee JJ (2015) Second-generation PLINK: rising to the challenge of larger and richer datasets. Gigascience 4:7 10.1186/s13742-015-0047-8 [PubMed: 25722852]

Compston J (2013) Obesity and bone. Curr Osteoporos Rep 11:30–35. 10.1007/s11914-012-0127-y [PubMed: 23288547]

Deng HW et al. (2000) Determination of bone mineral density of the hip and spine in human pedigrees by genetic and lifestyle factors. Genet Epidemiol 19:160–177. 10.1002/1098-2272(200009)19:2<160:AID-GEPI4>3.0.CO;2-H [PubMed: 10962476]

Dickinson ME et al. (2016) High-throughput discovery of novel developmental phenotypes. Nature 537:508–514. 10.1038/nature19356 [PubMed: 27626380]

Duncan EL et al. (2011) Genome-wide association study using extreme truncate selection identifies novel genes affecting bone mineral density and fracture risk. PLoS Genet 7:e1001372 10.1371/journal.pgen.1001372 [PubMed: 21533022]

ENCODE Project Consortium (2011) A user's guide to the encyclopedia of DNA elements (ENCODE). PLoS Biol 9:e1001046 10.1371/journal.pbio.1001046 [PubMed: 21526222]

Ensrud KE et al. (1997) Body size and hip fracture risk in older women: a prospective study. Study of Osteoporotic Fractures Research Group. Am J Med 103:274–280. 10.1016/s0002-9343(97)00025-9 [PubMed: 9382119]

Estrada K et al. (2012) Genome-wide meta-analysis identifies 56 bone mineral density loci and reveals 14 loci associated with risk of fracture. Nat Genet 44:491–501. 10.1038/ng.2249 [PubMed: 22504420]

Fall T, Ingelsson E (2014) Genome-wide association studies of obesity and metabolic syndrome. Mol Cell Endocrinol 382:740–757. 10.1016/j.mce.2012.08.018 [PubMed: 22963884]

Genomes Project C et al. (2010) A map of human genome variation from population-scale sequencing. Nature 467:1061–1073. 10.1038/nature09534 [PubMed: 20981092]

Gimble JM, Robinson CE, Wu X, Kelly KA (1996) The function of adipocytes in the bone marrow stroma: an update. Bone 19:421–428 [PubMed: 8922639]

Gomez-Ambrosi J, Rodriguez A, Catalan V, Fruhbeck G (2008) The bone-adipose axis in obesity and weight loss. Obes Surg 18:1134–1143. 10.1007/s11695-008-9548-1 [PubMed: 18563500]

Gonnelli S, Caffarelli C, Nuti R (2014) Obesity and fracture risk. Clin Cases Miner Bone Metab 11:9–14. 10.11138/ccmbm/2014.11.1.009 [PubMed: 25002873]

GTEx Consortium (2013) The Genotype-Tissue Expression (GTEx) project. Nat Genet 45:580–585. 10.1038/ng.2653 [PubMed: 23715323]

Guo Y et al. (2011) The fat mass and obesity associated gene, FTO, is also associated with osteoporosis phenotypes. PLoS ONE 6:e27312 10.1371/journal.pone.0027312 [PubMed: 22125610]

Haslam DW, James WP (2005) Obesity Lancet 366:1197–1209. 10.1016/S0140-6736(05)67483-1 [PubMed: 16198769]

Hsu YH et al. (2006) Relation of body composition, fat mass, and serum lipids to osteoporotic fractures and bone mineral density in Chinese men and women. Am J Clin Nutr 83:146–154. 10.1093/ajcn/83.1.146 [PubMed: 16400063]

Hu Y et al. (2018) Identification of novel potentially pleiotropic variants associated with osteoporosis and obesity using the cFDR method. J Clin Endocrinol Metab 103:125–138. 10.1210/jc.2017-01531 [PubMed: 29145611]

Kemp JP et al. (2017) Identification of 153 new loci associated with heel bone mineral density and functional involvement of GPC6 in osteoporosis. Nat Genet 49:1468–1475. 10.1038/ng.3949 [PubMed: 28869591]

Kim SK (2018) Identification of 613 new loci associated with heel bone mineral density and a polygenic risk score for bone mineral density, osteoporosis and fracture. PLoS ONE 13:e0200785 10.1371/journal.pone.0200785 [PubMed: 30048462]

Konstantopoulos S (2006) Fixed and mixed effects models in meta-analysis. IZA Discussion Paper No. 2198. https://ssrn.com/abstract=919993

Liu YZ et al. (2009) Powerful bivariate genome-wide association analyses suggest the SOX6 gene influencing both obesity and osteoporosis phenotypes in males. PLoS ONE 4:e6827 10.1371/journal.pone.0006827 [PubMed: 19714249]

Locke AE et al. (2015) Genetic studies of body mass index yield new insights for obesity biology. Nature 518:197–206. 10.1038/nature14177 [PubMed: 25673413]

Looker AC, Frenk SM (2015) Percentage of adults aged 65 and over with osteoporosis or low bone mass at the femur neck or lumbar spine: United States, 2005–2010. Division of Health and Nutrition Examination Surveys. November 2015. https://www.cdc.gov/nchs/data/hestat/osteoporsis/osteoporosis2005_2010.htm

Maes HH, Neale MC, Eaves LJ (1997) Genetic and environmental factors in relative body weight and human adiposity. Behav Genet 27:325–351 [PubMed: 9519560]

Manabe N et al. (2001) Connection between B lymphocyte and osteoclast differentiation pathways. J Immunol 167:2625–2631 [PubMed: 11509604]

Medina-Gomez C et al. (2018) Life-course genome-wide association study meta-analysis of total body BMD and assessment of age-specific effects. Am J Hum Genet 102:88–102. 10.1016/j.ajhg.2017.12.005 [PubMed: 29304378]

Morris JA et al. (2019) An atlas of genetic influences on osteoporosis in humans and mice. Nat Genet 51:258–266. 10.1038/s41588-018-0302-x [PubMed: 30598549]

Mullin BH et al. (2018) Expression quantitative trait locus study of bone mineral density gwas variants in human osteoclasts. J Bone Miner Res 33:1044–1051. 10.1002/jbmr.3412 [PubMed: 29473973]

Notelovitz M (1993) Osteoporosis: screening, prevention, and management. Fertil Steril 59:707–725 [PubMed: 8458485]

O'Rourke RW, White AE, Metcalf MD, Winters BR, Diggs BS, Zhu X, Marks DL (2012) Systemic inflammation and insulin sensitivity in obese IFN-gamma knockout mice. Metab Clin Exp 61:1152–1161. 10.1016/j.metabol.2012.01.018 [PubMed: 22386937]

Pei YF et al. (2014) Meta-analysis of genome-wide association data identifies novel susceptibility loci for obesity. Hum Mol Genet 23:820–830. 10.1093/hmg/ddt464 [PubMed: 24064335]

Pischon T et al. (2008) General and abdominal adiposity and risk of death in Europe. N Engl J Med 359:2105–2120. 10.1056/NEJMoa0801891 [PubMed: 19005195]

Pruim RJ et al. (2010) LocusZoom: regional visualization of genome-wide association scan results. Bioinformatics 26:2336–2337. 10.1093/bioinformatics/btq419 [PubMed: 20634204]

Purcell S et al. (2007) PLINK: a tool set for whole-genome association and population-based linkage analyses. Am J Hum Genet 81:559–575. 10.1086/519795 [PubMed: 17701901]

Rexrode KM et al. (1998) Abdominal adiposity and coronary heart disease in women. JAMA 280:1843–1848 [PubMed: 9846779]

Rivadeneira F et al. (2009) Twenty bone-mineral-density loci identified by large-scale meta-analysis of genome-wide association studies. Nat Genet 41:1199–1206. 10.1038/ng.446 [PubMed: 19801982]

Tan LJ et al. (2015) Bivariate Genome-Wide Association Study Implicates ATP6V1G1 as a Novel Pleiotropic Locus Underlying Osteoporosis and Age at Menarche. J Clin Endocrinol Metab 100:E1457–1466. 10.1210/jc.2015-2095 [PubMed: 26312577]

The Women's Health Initiative Study Group (1998) Design of the Women's Health Initiative clinical trial and observational study. The Women's Health Initiative Study Group Control Clin Trials 19:61–109 [PubMed: 9492970]

Ward LD, Kellis M (2012) HaploReg: a resource for exploring chromatin states, conservation, and regulatory motif alterations within sets of genetically linked variants. Nucleic Acids Res 40:D930–934. 10.1093/nar/gkr917 [PubMed: 22064851]

Zaitlen N, Kraft P, Patterson N, Pasaniuc B, Bhatia G, Pollack S, Price AL (2013) Using extended genealogy to estimate components of heritability for 23 quantitative and dichotomous traits. PLoS Genet 9:e1003520 10.1371/journal.pgen.1003520 [PubMed: 23737753]

Zhang L, Bonham AJ, Li J, Pei YF, Chen J, Papasian CJ, Deng HW (2009a) Family-based bivariate association tests for quantitative traits. PLoS ONE 4:e8133 10.1371/journal.pone.0008133 [PubMed: 19956578]

Zhang L et al. (2014a) Multistage genome-wide association meta-analyses identified two new loci for bone mineral density. Hum Mol Genet 23:1923–1933. 10.1093/hmg/ddt575 [PubMed: 24249740]

Zhang L, Li J, Pei YF, Liu Y, Deng HW (2009b) Tests of association for quantitative traits in nuclear families using principal components to correct for population stratification. Ann Hum Genet 73:601–613. 10.1111/j.1469-1809.2009.00539.x [PubMed: 19702646]

Zhang L, Pei YF, Fu X, Lin Y, Wang YP, Deng HW (2014b) FISH: fast and accurate diploid genotype imputation via segmental hidden Markov model. Bioinformatics 30:1876–1883. 10.1093/bioinformatics/btu143 [PubMed: 24618466]

Zhang L, Pei YF, Li J, Papasian CJ, Deng HW (2009c) Univariate/multivariate genome-wide association scans using data from families and unrelated samples. PLoS ONE 4:e6502 10.1371/journal.pone.0006502 [PubMed: 19652719]

Zhao LJ, Liu YJ, Liu PY, Hamilton J, Recker RR, Deng HW (2007) Relationship of obesity with osteoporosis. J Clin Endocrinol Metab 92:1640–1646. 10.1210/jc.2006-0572 [PubMed: 17299077]

Zheng HF et al. (2015) Whole-genome sequencing identifies EN1 as a determinant of bone density and fracture. Nature 526:112–117. 10.1038/nature14878 [PubMed: 26367794]

Zhu Z et al. (2018) Causal associations between risk factors and common diseases inferred from GWAS summary data. Nat Commun 9:224 10.1038/s41467-017-02317-2 [PubMed: 29335400]
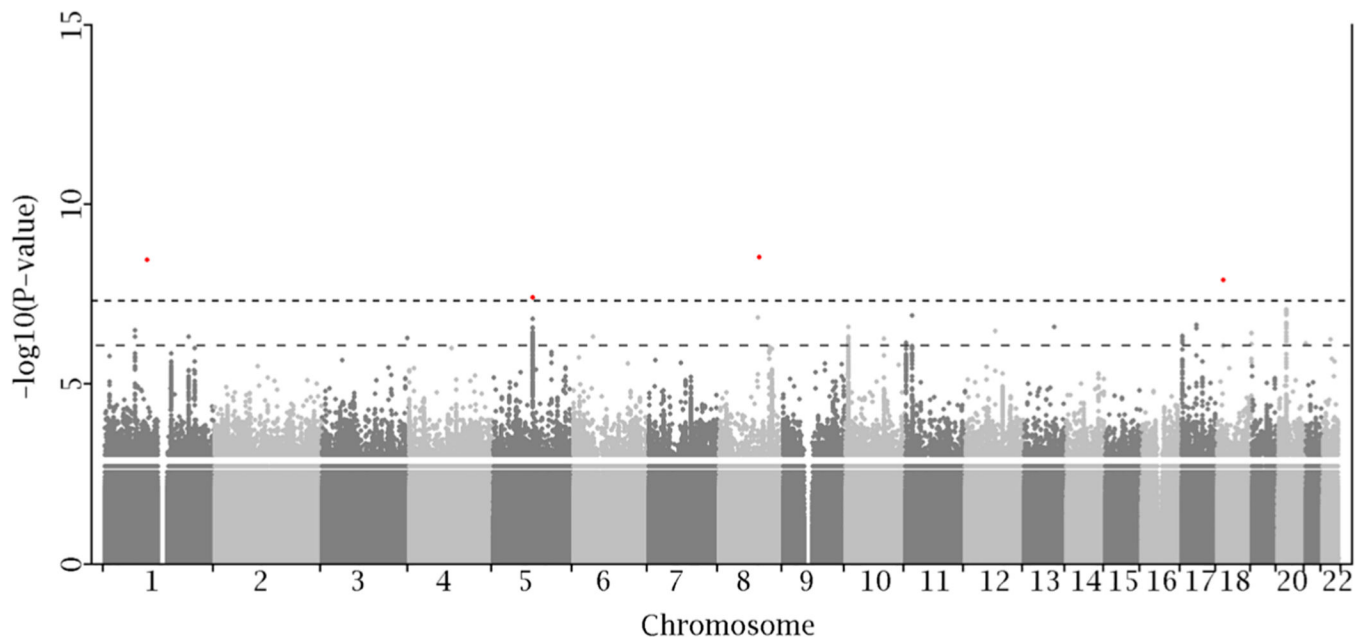
Fig. 1.
Manhattan plot of the bivariate meta-analysis. The results from the bivariate analysis are plotted against the position on each of the 22 chromosomes. The black dashed line indicates the threshold for genome wide significance level ($a = 5.0 \times 10^{-8}$). The gray dashed line indicates the threshold for suggestive significance level ($a = 1.0 \times 10^{-6}$)
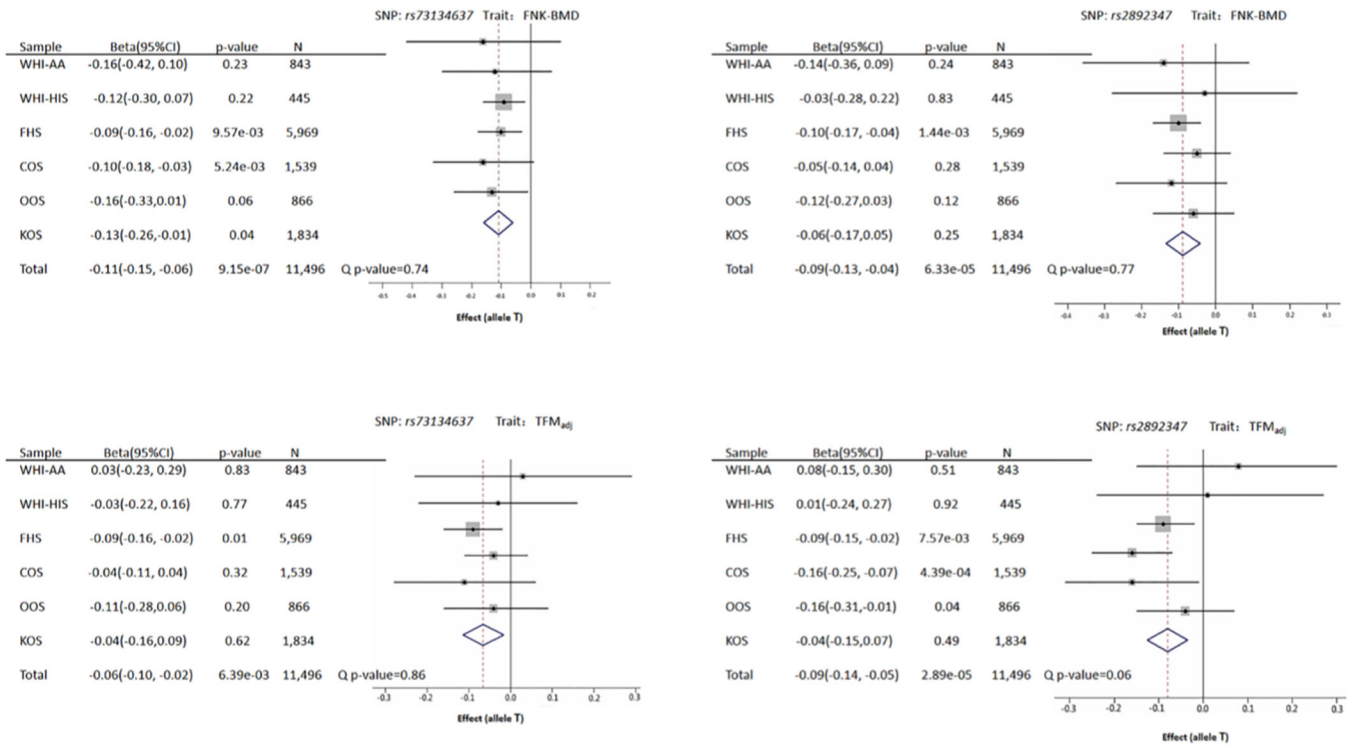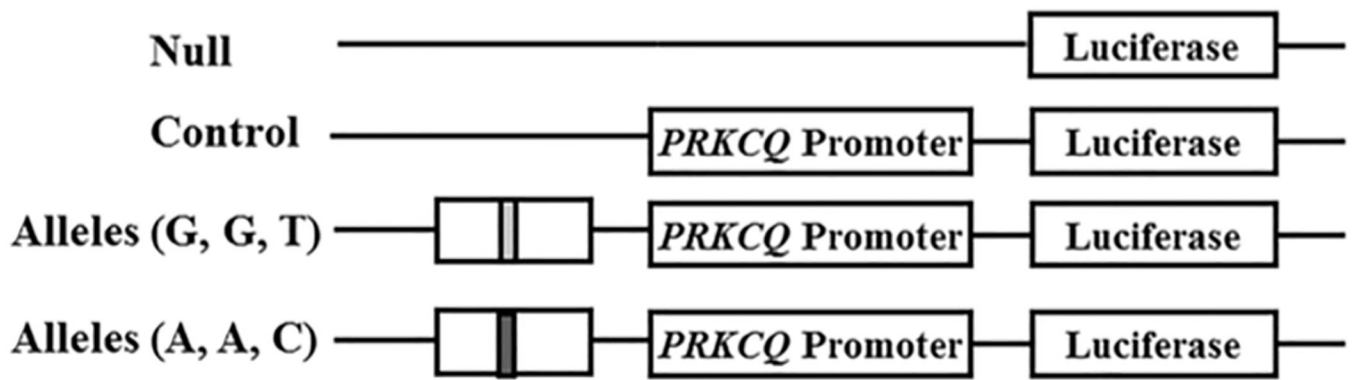
Fig. 2.

Forest plot of *rs73134637* and *rs2892347* meta-analysis. Regression coefficient (beta) and its 95% confidence interval (CI) are presented in un-transformed estimates from individual studies. "Total" refers to the combined meta-analysis. $Q\, p$ value represents Cochran's $Q\, p$ value, which did not show evidence of heterogeneity at any SNP
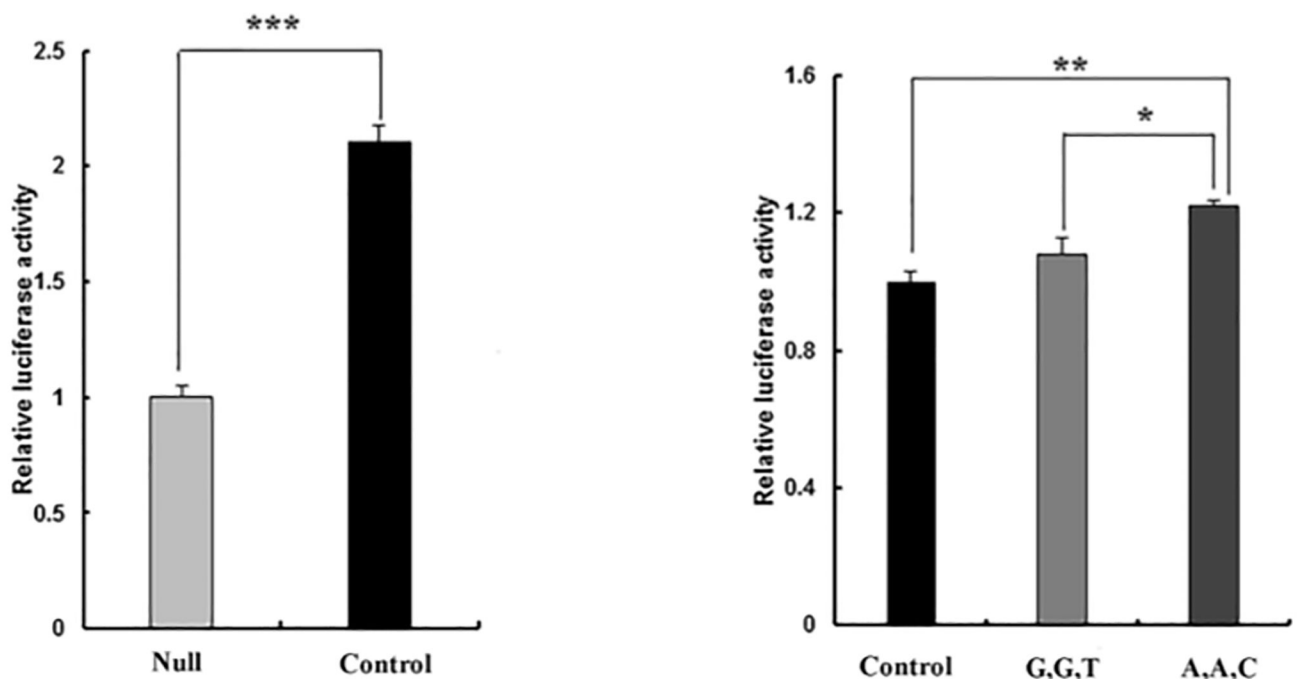
Fig. 3.
Dual-luciferase reporter assay result. The pGL3-PRKCQ-Promoter vector was set as a control. Sequence construct containing either trait-raising alleles (*rs11254759*-G, *rs11254758*-G, *rs11254760*-T) or trait-lowering alleles (*rs11254759*-A, *rs11254758*-A, *rs11254760*-C) was inserted upstream of the gene promoter. Four replicates were conducted under each of the three conditions. Compared to the null pGL3-basic vector, the vector containing the *PRKCQ* promoter increased luciferase expression ($p = 4.60 \times 10^{-7}$). Both trait-raising allele construct and trait-lowering allele construct significantly increase luciferase activity ($p = 0.10$ and 0.002, respectively), suggesting that the sequence containing three variants improves *PRKCQ* promoter activity. Between the two allele

constructs, the expression of trait-raising alleles is significantly higher than that of trait-lowering alleles ($p = 0.01$), implying that the regulation is related to different alleles

Table 1

Basic characteristics of the studied samples

Sample	Source	Anc	N	Female (%)	Age	Weight (kg)	Height (cm)	TFM (kg)	TLM (kg)	FNK-BMD (g/cm²)
OOS	In-house	EUR	866	48.2	50.4(18.2)	81.5 (17.9)	171.0 (9.7)	12.2 (5.9)	28.0 (6.3)	0.81 (0.14)
KCOS	In-house	EUR	1834	23.3	51.5 (13.7)	75.0(17.3)	166.2 (8.4)	11.0 (5.9)	25.1 (5.4)	0.80 (0.15)
COS	In-house	EAS	1539	50.6	34.7(13.4)	60.3 (10.6)	164.3 (8.2)	6.5 (3.1)	21.4 (4.0)	0.81 (0.13)
FHS	dbGAP	EUR	5969	58.1	55.3 (13.6)	82.5 (17.5)	167.8 (9.9)	15.1 (5.7)	25.8 (5.6)	0.89 (0.16)
WHI-HIS	dbGAP	AMR	445	100	60.1 (7.5)	72.7 (14.7)	158.2 (5.6)	15.9 (5.8)	19.3 (2.6)	0.73 (0.12)
WHI-AA	dbGAP	AFR	843	100	61.2(7.3)	78.8(16.9)	162.7 (5.8)	17.0 (6.4)	20.7 (2.9)	0.83 (0.14)

A total of six samples were collected. Three were from in-house studies, and the other three were accessed through the dbGAP

Data presented as mean (SD). Sample size (*N*) after quality control was reported

OOS Omaha osteoporosis study, *KCOS* Kansas City osteoporosis study, *COS* China osteoporosis study, *FHS* Framingham Heart Study, *WHI-AA and WHI-HIS* Women's Health Initiative (WHI) cohort African-American subsample and Hispanic subsample. Anc., ancestral population. *Anc.*, ancestral population, *EUR* European ancestral population, *EAS* East Asian ancestral population, *AER* African ancestral population, *AMR* Admixed American ancestral population, *TFM* trunk fat mass, *TLM* trunk lean mass, *FNK-BMD* femoral neck bone mineral density

Table 2

The main results of *rs73134637*, *rs2892347* and *rs11254759*

SNP	CHR	POS	Locus	EA	OA	Bivariate meta-analysis				UKB cross-replication			
						Beta-BMD	Beta-TFM$_{adj}$	Bivariate p	N	Trait	Beta	p	N
rs73134637	12	68,922,645	12q15	T	C	−0.11	−0.06	3.45×10^{-7}	11,496	OP1	7.95×10^{-4}	0.06	410,289
										TFP	−0.05	0.03	492,388
rs2892347	10	6,838,849	10p14	T	G	−0.09	−0.09	2.63×10^{-7}	11,496	OP2	9.97×10^{-4}	0.02	383,478
										BMI	−0.04	4.61×10^{-3}	499,520
rs 11254759	10	6,857,307	10p14	G	A	0.08	0.09	9.49×10^{-7}	11,496	OP2	$−1.02 \times 10^{-3}$	0.02	382,462
										BMI	0.03	0.02	492,674

Beta is the regression coefficient of normalized phenotypic residual on the effect allele A

POS genomic position based on GRCH37 genome assembly, *EA* effect allele, *OA* other allele, *OOS* Omaha osteoporosis study, *KCOS* Kansas City osteoporosis study, *FHS* Framingham Heart Study, *WH1*-*H1S* Women's Health Initiative (WHI) cohort Hispanic subsample, *UKB* UK Biobank, *TFM$_{adj}$* trunk fat mass adjusted by trunk lean mass, *BMD* bone mineral density, *BMI* body mass index, *TFP* trunk fat percentage, *OP1* osteoporosis without pathological fracture, *OP2* osteoporosis